DIRECT GEOREFERENCING OF TLS IN SURVEYING OF COMPLEX SITES

Marco Scaioni

Politecnico di Milano – Polo Regionale di Lecco, Dept. I.I.A.R., via M. d'Oggiono 18/a, 23900 Lecco, Italy
e-mail: marco.scaioni@polimi.it

KEY WORDS: Terrestrial Laser Scanning, Direct Georeferencing, Architectural Surveying, Civil Surveying, Tunnel

ABSTRACT:

The high powerfulness of TLS technique for quick 3D data acquisition is extending its use to many fields. To further reduce the surveying time and to simplify all operational tasks, the TLS *direct georeferencing* may be a very suitable approach instead of the technique based on ground control points (*targets*). This chance is allowed by the most part of existing instruments, as a default or as an optional capability. The paper describes the geometric model involved in the direct georeferencing, considering scanners mounted either in vertical and in tilted position. Secondly, an analysis of errors affecting laser scanners measurement is proposed. The total error budget results from the propagation of errors due to intrinsic measurements and to the adopted georeferencing technique. Here errors connected to the instrument setup needed to get direct georeferencing are analized. Finally, a simulation finalized to define the achievable accuracy in 3D point measurement according to different sets of instrumental parameters is proposed. Furthermore, simulated data have been compared to a real case of data acquisition performed by means of both direct georeferencing and by the use of ground control points.

1. INTRODUCTION

Terrestrial Laser Scanning (TLS) is currently a powerful acquisition technique allowing to collect a large amount of 3D data in a relatively short time. The basic information which is directly collected from each scan position is the so called *point cloud*, made up of all 3D points of the surveyed surface in correspondence of nodes of a regular spherical grid around the instrument. Coordinates are integrated by other kinds of data: at least the *intensity* of laser responce is registered, but also RGB data can be achieved thank to an internal or external calibrated digital camera.

The laser scanning approach is widely suitable for the acquisition of large objects in architectural, civil engineering and land monitoring fields, requiring in such cases the collection of several scans that must be put together in a common reference system. The registration of each scan into a reference system is usually performed by means of *ground control points* (GCPs) in a similar way that is done in photogrammetry. The number of GCPs to be measured for each scan consists in a minimum of 3, but a higher number is strongly recomended to increase the numerical stability and reliability of the solution. Yet some GCPs could be shared among more scans, their numbers will increase very sharply in case of surveying of large sites. However, this method is largely suitable for the most cases of TLS applications due to its semplicity and to the achievable high accuracy in point cloud georeferencing (see par. 4), if a stable geometric configuration for the ground constraints is established. Nevertheless, data acquisition and commercial processing SWs are prevalently based on this approach.

On the other hand, there are some applications where the use of GCP-based georeferencing methods is not completely suitable because of technical, economical or operational reasons. Contexts where alternative georeferencing methods are invoked for can be classified as follows:

1. objects featuring a prevalent dimension (e.g. tunnels, roads, etc.) where the geometric shape of the object does not allow to establish a stable set of GCPs, or where the large number of scans that have to be captured would make too expensive their positioning;
2. applications where large portions of land have to be acquired at low resolution for the purpose of landscape or city modeling;
3. when the positioning of GCPs is however very complex or not possible at all.

In literature three alternative methods are proposed to perform scan georeferencing, all featuring the possibility of reducing GCPs to the minimum configuration needed to insert the whole point cloud into the ground reference system. The first group collects all algorithms for *surface matching* (see Grün & Akca, 2004 for a review), allowing pairwise co-registration of scans on the basis of a shared portion of the captured surface. Starting from a scan assumed as reference, all the other ones are joined up as far as the whole point cloud is co-registered. Finally some GCPs are inserted for ground georeferencing. The main drawback of this approach is that scans must share large portions featuring a texture rich of details recognizable by *surface matching* algorithms.

To exploit the higher accuracy of target measurement, a method based on the *simultaneous block adjustment* of all scans has been proposed (Scaioni & Forlani, 2003). In Ullrich *et al.* (2003) a *hibrid multi-station adjustment* comprehending 3D-views and digital images captured by a camera co-registered to the TLS has been presented. Advantages of such methods are those typical of photogrammetric block triangulation, resulting in a strong reduction of GCPs' numbers, which are replaced by *tie points*. Limitations are: scans should share enough tie points; an accurate project of scans is required to guarantee a stable geometry to the block; a highly-experienced operator is needed to plan ground and tie point positions.

In this paper we would like to focus on a third solution, which is usually addressed to in literature as *direct georeferencing*. By this approach a TLS becomes very close to a *motorized total station*: it can be mounted over a tribrach provided of optical plummet and of a level bubble, allowing centering over a known point and levelling. Thanks to a telescope (see Fig. 1) or by backsighting a target, the orientation in the horizontal plane can be carried out. In Lichti & Gordon (2004) a complete analysis of currently available scanners enabling direct georeferencing is reported.

At time of writing and as far as the author's knowledge, some data acquisition SWs encompass the possibility of direct georeferencing, even though this is limited to a well established procedure only. Here the geometric model involved in this task is described and an operational method to get direct georeferencing of scans is proposed (par. 3). Furthermore, an analysis of error sources related to laser scanning data is reported, so that the achievable accuracies by different methods can be compared (par. 4). Finally a simulated test and a practical case study concerning the surveying of an ancient church afforded by different approaches is reported.
In par. 2 some basic fundamentals concerning reference systems adopted in the following of the paper are given.

Fig. 1 – The scanner Riegl LMS-Z420i equipped by the telescope for TLS's azimuth direct orientation and by the device enabling the tilt-mounting.

2. BACKGROUND ON 3D-SCAN GEOREFERENCING

The problem of scan registration is usually addressed through the definition of 2 reference systems (RS): the *intrinsic* and the *ground* RS. With reference to Figure 2 they are analyzed in the following paragraphs.

2.1 Intrinsic reference system

Usually a laser scanner performs the measurement of a large point cloud in a very short time (up to 12k points per second in case of the fastest existing TLS). For each laser point a range measurement (ρ_m) and an intensity value (I) are collected; these data may be integrated by RGB information in case a digital camera is co-registered to the scanner. Furthermore, the horizontal rotation angle (α_m) and the vertical attitude angle (θ_m) are registered for each measured point, allowing its determination in the *intrinsic reference system* (IRS) of a given scan position. In practice, if more than one scan are captured from the same stand-point without altering the TLS position and attitude, all resulting 3D-views will be referred into the same IRS.
By construction, the laser scanner axes are not perfectly aligned, so that these differences have to be corrected in order to transfer the measured spherical coordinates (ρ_m,α_m,θ_m) into the IRS (ρ,α,θ). The geometric model adopted to perform this correction should be given by TLS technical documentation, but this does not happen for all instruments. On the other hand, each laser scanner model is usually provided by its own software for data acquisition control, which directly performs the correction of 3D point coordinates into the IRS. In the following we refer to spherical coordinates of a point through the *vector of measurements* $\rho = [\rho\ \alpha\ \theta]^T$. The transformation from spherical coordinate ρ to cartesian coordinates is given by the following equations:

$$x = \begin{bmatrix} x \\ y \\ z \end{bmatrix} = \begin{bmatrix} \rho \cdot \cos\theta\cos\alpha \\ \rho \cdot cos\theta\sin\alpha \\ \rho \cdot sin\theta \end{bmatrix} \quad (1)$$

2.2 Ground reference system

The *ground reference system* (GRS) is shared between more than one scan. To trasform each scan from its own IRS into a GRS a 3D roto-translation is to be computed on the basis of common control points (or features). This operation is called *scan co-registration*. Given the vector X storing coordinates of a point in the GRS, the trasformation from the IRS can be expressed by introducing the *rotation matrix* **R** and the vector O_1 expressing the origin of the IRS with respect to the GRS:

$$X = \mathbf{R}x + O_1 \quad (2)$$

The rotation matrix **R** can be parameterized by *cardanic angles* (ω,φ,κ) as commonly done in photogrammetry.
Concerning materialization of a GRS, this can be done by a set of control points with known coordinates, or by considering a scan as reference for co-registering all the others that overlap to it.
Usually a GRS corresponds to a given geodetic RS. In the architectural field, due to limitation of the survey site extension to a few hundred meter, a local planar approximation for the height reference surface is adopted. The resulting GRS features the z axis aligned to the mean vertical direction in the interested area and the xy plane orthogonal to it.

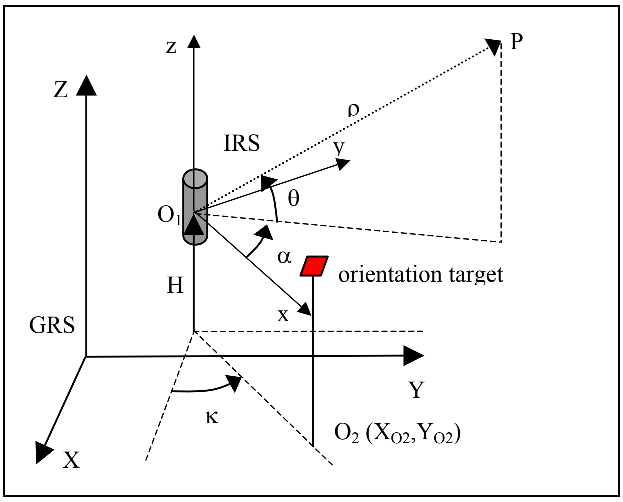

Figure 2 – Ground and Intrinsic RS of a scan position.

2.3 Indirect and direct georeferencing

The term *georeferencing* means the computation of **R** and O_1 for each scan position. The widespread technique to do this is based on registering each scan to the GRS by means of a set of GCPs materialized by *targets* or by natural features. Thanks to the knowledge of a minimum of 3 GCPs that can be measured in the scan to be georeferenced, all 6 parameters of the roto-translation can be computed by a resection technique. In practice, the GCPs' number should be increased in order to push up the redundancy. Being this problem not linear, usually an algorithm which does not require any approximations for the unknowns is applied; in literature a large variety of these methods are reported (see Beinat & Crosilla, 2001). To cope with possible outliers and to automatically find corresponding points on the scan and the ground, the RANSAC algorithm is widely used (Fischler & Bolles, 1981). Finally, once a set of good GCPs has been established, a *least squares* based algorithm is applied to exploit the data redundancy – if available – and to evaluate the accuracy of the estimated solution.

Even though in literature different methods based on a block adjustment for computing both **R** and O_1 of each scan have been proposed (see par. 1), their use is still very limited in practitioners' applications.

The second strategy to perform the scan georeferencing is that based on the so called *direct* approach. The most part of existing TLS can be *directly georeferenced*, meaning that the sensor can be optically centered over a known point and levelled, while the remaining degree-of-freedom can be fixed by orienting the IRS system toward a known point. The last task can be performed by using a telescope mounted on the laser scanner or by scanning a *backsighting target*. In the sequel the geometric model which is usually adopted for *direct georeferencing* is presented, considering also the case of a TLS mounted in tilted position.

The chance of success of such a method will depend obviously on the final accuracy of 3D point cloud coordinates measurement. To this aim, at par. 4 an analysis of errors affecting both indirect and direct georeferencing methods is reported.

3. GEOMETRIC MODEL FOR DIRECT GEOREFERENCING

The simplest method to get *direct georeferencing* of a scan is based on the possibility of centering the TLS over a know point by an optical plummet, to level the instrumental basement and to fix an horizontal direction by means of a telescope which is calibrated with respect to the IRS. Disregarding specific practical solutions adopted in currently available TLSs and possible user-made improvements, here we would like to focus on the general geometric model.

The basic geometric model describing a TLS which can be oriented by a telescope is similar to that describing a classical theodolite. The scanner is stationed over a known point in a given GRS while the z axis of its own IRS is put vertical. Being known the vector H from the stationing point to the origin O_1 of the IRS from calibration or from mechanical drawings, coordinates of O_1 in the GRS can be easily derived.

The telescope is usually blocked over the TLS scanner head and can be rotated in the xz plane defined by the IRS. By collimating a point O_2 having planimetric known coordinates in the GRS (X_{O2},Y_{O2}) also the direction of the x axis of the IRS can be fixed and then the horizontal angle κ constrained. The IRS will result rotated around the z axis of an angle κ with respect to the GRS; for this reason, we refer to a generic point in the IRS by vector x_κ. The transformation from IRS to the GRS is given by the expression:

$$X = \mathbf{R}_\kappa x_\kappa + O_1 \tag{3}$$

where the rotation matrix $\mathbf{R}_\kappa$ will define the rotation κ from the IRS to the GRS:

$$\mathbf{R}_\kappa = \begin{bmatrix} \cos\kappa & -\sin\kappa & 0 \\ \sin\kappa & \cos\kappa & 0 \\ 0 & 0 & 1 \end{bmatrix} \tag{4}$$

In eq. (3) the only parameter which is still unknown is the angle κ, that can be computed as follows:

$$\kappa = \operatorname{atan}\frac{Y_{O_2} - Y_{O_1}}{X_{O_2} - X_{O_1}} \tag{5}$$

Let us now introduce into the model the chance of rotating the scanner in the vertical plane, task which can be performed by a mechanical device enabling a tilt mounting at some fixed angular steps (see an example in Fig. 1). This possibility is required when the instrument has a limited vertical FoV and an object positioned upwards has to be scanned.

We consider the new rotation ϕ around the y axis; only a set of discrete values $\phi = \{\phi_1, \phi_2, ..., \phi_n\}$ for this angle can be setup on the tilt-mounting device.

The order of rotations introduced so far follows the operational procedure used for TLS backsighting by means of a telescope: firstly the scanner is stationed in vertical position (ϕ=0); secondly is rotated around the z axis in order to collimate the *backsighting target* by the telescope; finally it is tilted around the y axis.

To consider also the rotation in the vertical plane, a new matrix $\mathbf{R}_\phi$ is introduced:

$$\mathbf{R}_\phi = \begin{bmatrix} \cos\phi & 0 & \sin\phi \\ 0 & 1 & 0 \\ -\sin\phi & 0 & \cos\phi \end{bmatrix} \tag{6}$$

Coordinates of a point in the IRS considering also the second rotation ($x_{\kappa\phi}$) are related to coordinate after the first rotation only (x_κ) by the expression:

$$x_{\kappa\phi} = \mathbf{R}_\phi^T x_\kappa \tag{7}$$

Unfortunately, the introduction in eq. (3) of the value of x_κ derived from (7) is not enough for modelling what really happens in mechanical devices for tilt-mounting, because the rotation axis is usually not centered in the origin O_1 of the IRS, but may be shifted in x (seldom) and z direction (frequently) by eccentricities e_x and e_z (see Fig. 3). Consequently eq. (7) must be corrected by keeping into account the effect of the eccentric rotation:

$$x_{\kappa\phi} = \mathbf{R}_\phi^T x_\kappa + e \tag{8}$$

The *eccentricity vector e* is defined as follows:

$$e=\begin{bmatrix} e_x - r_e\cos(\phi+\gamma) \\ 0 \\ e_z - r_e\sin(\phi+\gamma) \end{bmatrix} \qquad r_e=\sqrt{e_x^2+e_z^2}\ ;\ \gamma=\text{atan}(e_z/e_x) \quad (9)$$

Values of e_x and e_z can be derived from mechanical drawings of TLS or from scanner calibration.
Finally, by computing vector x_κ from eq. (8) and by introducing it into eq. (3), you get the new expression of the transformation from the IRS ($x_{\phi\kappa}$) to the GRS in case of tilt-mounting:

$$X=\mathbf{R}_\kappa x_\kappa + O_I = \mathbf{R}_\kappa \mathbf{R}_\phi (x_{\kappa\phi}-e)+O_I = \mathbf{R}_{\phi\kappa}(x_{\kappa\phi}-e)+O_I \quad (10)$$

where $\mathbf{R}_{\phi\kappa}=\mathbf{R}_\kappa\cdot\mathbf{R}_\phi$.
The proposed method still holds in case instead of sighting a target by a telescope, the TLS allows to scan a structured target and to adopt its estimated centroid position for the orientation of *x* axis.

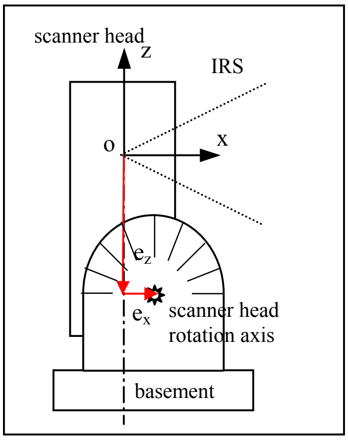

Fig. 3 – Geometric scheme of a device for TLS tilt-mounting in the general case

4. ANALYSIS OF THE UNCERTAINTY IN TLS MEASUREMENTS

From a general point of view, the uncertainty of a 3D point coming from laser scanning acquisition arises from several sources, some connected to the intrinsic measurements (i) - range and angles - and the others to the adopted georeferencing procedure (ii). This is only a rough classification, which however may help to evaluate the final uncertainty according to a given georeferencing method. In reality, errors on measurements also affect georeferencing, as happens e.g. when a 3D resection method is used for registration, being this based on target measurement suffering from intrinsic errors as well.
All possible error sources are briefly reported in Table 1 with expressions for their evaluation; the contribute of each error source is represented into a specific covariance matrix. The approach proposed by Lichti & Gordon (2004) has been mainly followed.
Group (i) encompasses the effect of *noise* in measurements and the *laser beamwidth*. The total contribute of these errors is accounted for in the covariance matrix $\mathbf{C}_{\mathbf{int}}$:

$$\mathbf{C}_{\mathbf{int}}=\mathbf{C}_{\mathbf{b}}+\mathbf{C}_{\mathbf{obs}} \quad (11)$$

where expressions for matrices on the right are reported in Table 1. In the next sub-paragraphs an analysis of errors of group (ii) is reported according to both direct and indirect georeferencing methods.

4.1 Errors in direct georeferencing

The error budget arises from the analysis of all error sources contributing to covariance propagation applied to eq. (10).
The covariance matrix $\mathbf{C_O}$ associated to vector O_I (position of the instrumental centre) will depend on the sum of two covariance matrices:

$$\mathbf{C_O}=\mathbf{C}_{\mathbf{net}}+\mathbf{C_H} \quad (12)$$

Firstly the covariance matrix of the ground stationing point $\mathbf{C}_{\mathbf{net}}$ must be considered; it can be taken from the adjustment of the geodetic network. In general this matrix is not diagonal, because in applications where direct georeferencing is applied poor redundant network schemes are often used and coordinates might be highly correlated. The second contribute is given by the uncertainty of vector *H* expressing the relative position of the instrumental centre with respect to the stationing point on the ground (Fig. 2). The resulting covariance matrix $\mathbf{C_H}$ is diagonal, made up of variances of *H*'s components. In the most cases, both planimetric components of *H* can be determined with a high accuracy from instrumental drawings, considering that errors due to centering will be deal with among setup errors. On the contrary, the instrumental height h_s must be evaluated every time on the field, introducing an error which cannot be neglected. A further error involving precision of network measurements is that related to the computation of azimuth by formula (5).
A second class of errors is that related to the instrumental setup, grouping stand-point and orientation target optical centering, levelling and manual point collimation to the backsight station (or scanning of a target over a known point). All these errors are included in the covariance matrix $\mathbf{C}_{\mathbf{set}}$.
The total covariance matrix of a 3D scanned point can be computed by the variance propagation law applied to (10):

$$\mathbf{C_X}=\mathbf{C_0}+\mathbf{J}_\rho(\mathbf{C}_{\mathbf{int}}+\mathbf{C}_{\mathbf{set}})\mathbf{J}_\rho^{\mathbf{T}}+\mathbf{J}_\kappa\mathbf{C}_\kappa\mathbf{J}_\kappa^{\mathbf{T}} \quad (13)$$

In formula (13) the uncertainty due to tilt-mounting angle ϕ and to both eccentricities e_x and e_z has been neglетted, because of the high accuracy of mechanical devices currently adopted to this aim.
Expressions of both jacobians in formula (13) are the following for the general case of tilted mount:

$$J_\rho=\frac{\partial X}{\partial x_{\kappa\phi}}\frac{\partial x_{\kappa\phi}}{\partial \rho}=\mathbf{R}_{\phi\kappa}\begin{bmatrix} \cos\theta\cos\alpha & -\rho\cos\theta\sin\alpha & -\rho\sin\theta\cos\alpha \\ \cos\theta\sin\alpha & \rho\cos\theta\cos\alpha & -\rho\sin\theta\sin\alpha \\ \sin\theta & 0 & \rho\cos\theta \end{bmatrix} \quad (14)$$

$$J_\kappa=\frac{\partial X}{\partial \kappa}=\frac{\partial \mathbf{R}_{\phi\kappa}}{\partial \kappa}(x_{\kappa\phi}-e) \quad (15)$$

4.2 Errors in georeferencing by resection

When applying a resection method for computing the georeferencing of a scan usually at least a small redundancy in observed GCPs exists and a standard l.s. estimation is applied. Thank to GCPs and their corresponding measured points in the IRS, a system can be established and solved for the 6 registration parameters of each scan. Moreover, variances of targets in object space could be introduced into the system as pseudo-observations if their values would not be negligible.

The uncertainty of the estimated parameters is given through the covariance matrix yielded during the l.s. procedure ($\mathbf{C}_{\mathbf{geo}}$), depending on the accuracy of targets in the IRS and possibly in the GRS, as well as on their geometric positions (on this subject see Gordon & Lichti, 2004).

Finally the positional uncertainty of a measured point (covariance matrix $\mathbf{C}_\mathbf{X}$) can be computed from error propagation through eq. (3), considering as stocastic variables either the estimated georeferencing parameters and the scanner measurements in vector ρ. The covariance matrix $\mathbf{C}_\mathbf{X}$ will result as:

$$\mathbf{C}_\mathbf{X} = \mathbf{J}_\mathbf{geo}\mathbf{C}_\mathbf{geo}\mathbf{J}_\mathbf{geo}^\mathbf{T} + \mathbf{J}_\rho\mathbf{C}_\mathbf{int}\mathbf{J}_\rho^\mathbf{T} \tag{16}$$

Error source	Uncertainty expression (1σ)	Meaning of parameters	Covariance matrix
measurements	$\sigma_\rho,\sigma_\alpha,\sigma_\theta$ (from manufacturers or from metrological tests)	σ_ρ = uncertainty of range $\sigma_\alpha,\sigma_\theta$ = uncertainties of horizontal and vertical angles m = # of averaged measurements (multi-scan)	$\mathbf{C}_\mathbf{obs}=\mathrm{diag}(\sigma_\rho^2,\sigma_\alpha^2,\sigma_\theta^2)/m$
laser beamwidth	$\sigma_b = \pm\delta/4$	δ = diameter of laser cross-section in angular units	$\mathbf{C}_\mathbf{b}=\mathrm{diag}(0,\sigma_b^2,\sigma_b^2)$
azimuth	$\sigma_\kappa = \pm\frac{\sqrt{2}\sigma_H}{d_{O_1O_2}}$	σ_H = mean planimetric uncertainty of network points	$\mathbf{C}_\kappa=[\sigma_\kappa^2]$
TLS and backsighting target centering	$\sigma_d = \pm\frac{\sqrt{2}\sigma_c}{d_{O_1O_2}}$	σ_c = mean centering uncertainty of a stationing points	$\mathbf{C}_\mathbf{set} = \begin{bmatrix} 0 & 0 & 0 \\ 0 & (\sigma_{IH}^2+\sigma_d^2+\sigma_p^2) & 0 \\ 0 & 0 & \sigma_{IV}^2 \end{bmatrix}$ or alternatively if the method of target backsighting has been used: $\mathbf{C}_\mathbf{set} = \begin{bmatrix} 0 & 0 & 0 \\ 0 & (\sigma_{IH}^2+\sigma_d^2+\sigma_{pc}^2) & 0 \\ 0 & 0 & \sigma_{IV}^2 \end{bmatrix}$
instrument levelling	$\sigma_{IH} = \pm\,\sigma_{IV}\tan\theta$ $\sigma_{IV} = \pm\,0.2\,v''$	σ_{IH}, σ_{IV} = uncertainties in horizontal and vertical angles related to the levelling v″ = level sensitivity	
pointing error by telescope	$\sigma_p = \pm\frac{60''}{M}$	M = telescope magnification	
pointing error by target backsighting	$\sigma_{pc} = \pm\frac{\Delta}{2\sqrt{3}}$	Δ = angular sampling interval in both α and θ	

Table 1 – Expressions of uncertainties of parameters involved in direct georeferencing of a TLS (from Licthi & Gordon, 2004).

4.3 Uncertainty in current practitioners' applications

We would like here to make some considerations about uncertainty in practical TLS surveying for civil engineering and cultural heritage recording. In case a simulation of point cloud accuracy is required before data capture, covariance matrices for computing error propagation are needed. A first group of these can be easily recovered, depending only on technical properties of adopted hardware (i.e. levelling bubble, backsighting telescope or target). Unfortunately, tools supplied by vendors to enable direct georeferencing (in many case not as default but optionally) are usually of low quality; in applications where the highest accuracy is required, they have to be replaced by improved user-made tools. However, the verticality of the main instrumental axis is the major source of error due to the fact that a *dual axis compensator* is not available yet in current TLSs, even though it is commonplace that it is becoming a standard in the future. In the context of the present research, some trials in a calibrated test-field are ongoing to the aim of evaluating the effective verticality error.

The accuracy of the geodetic network nodes, which directly influences the TLS positioning through the covariance matrix $\mathbf{C}_\mathbf{O}$, is completely application-depending. In the considered fields of application, redundant geodetic networks are seldom adopted, due to the shape of surveyed objects or to the large range of uncertainty which is commonly tolerated. In small networks the adoption of homogeneous values for st.dev.s of each vertex's coordinates is reasonably accepted; these values can be computed from the application of error propagation theory or from standard tables in case of well known network geometries (e.g. a traverse). If a more complex geodetic network has been used, as in the acquisition of very large settlements, values for $\mathbf{C}_\mathbf{O}$ could come from a l.s. simulation.

Considerations about uncertainty in range and angles measurements have been already made at par. 4.1. According to Lichti & Gordon (2004) and to Fröhlich & Mettenleiter (2004), we retain that values reported in technical reports are not enough reliable, but they should be derived from practical on-the-field test.

5. TWO EXAMPLES

In order to evaluate the uncertainty of 3D spoints measurements by applying different methods for scan georeferencing, we have performed two tests. The first one concerns the simulation of the covariance matrix of points in a typical configuration usually adopted in laser scanning data acquisition, according to some sets of instrumental parameters affecting the final accuracy. In a second test, a TLS surveying of an ancient church which was already carried out adopting georeferencing by resection has been recomputed by the direct technique.

5.1 Simulation of 3D point uncertainty in a typical configuration for data acquisition

Simulations have been computed by considering the geometric configuration in Figure 4, with the instrument mounted in vertical position and equipped by a telescope for azimuth orientation. Accuracy has been evaluated for 3D point coordinates in the range 12.5÷100 m of horizontal distance from instrument stand-point; two different vertical angles have been considered: θ_1=0° and θ_2=40°. Among all possible, only 6 combinations of parameters (see Fig. 5) have been tried, according to the following criteria: to test instruments featuring different accuracy in intrinsic measurements and laser beamwidth (i); to consider low (sets 1-2-3) and high (sets 4-5-6) quality tools for direct georeferencing, i.e telescope and level bubble (ii).

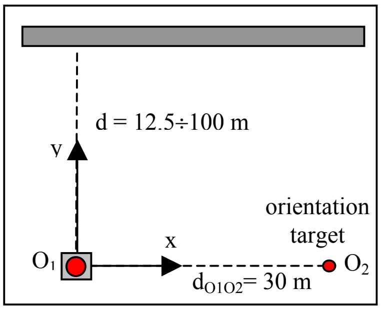

Fig. 4 – Geometric configuration for TLS data acquisition considered in the simulated test

	M=3, v=2′	M=30, v=20″
laser beam-width: 0.12 mrad σ_ρ= ± 5 mm $\sigma_{\alpha-\theta}$= ± 4 mgon	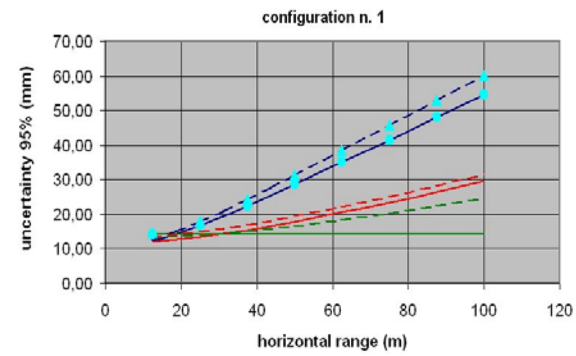	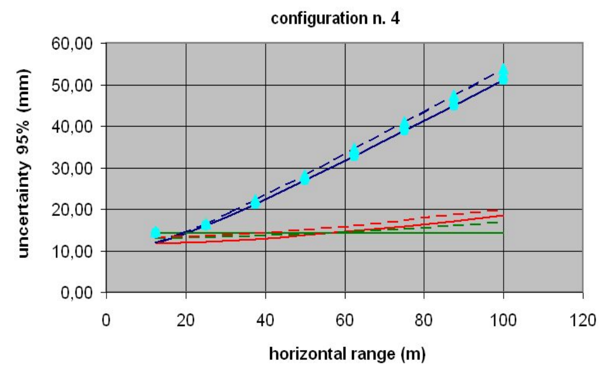
laser beam-width: 0.75 mrad σ_ρ= ± 10 mm $\sigma_{\alpha-\theta}$= ± 40 mgon	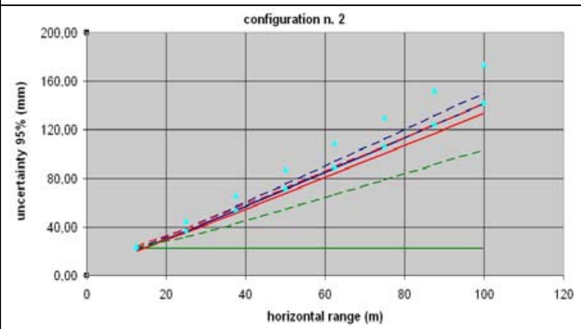	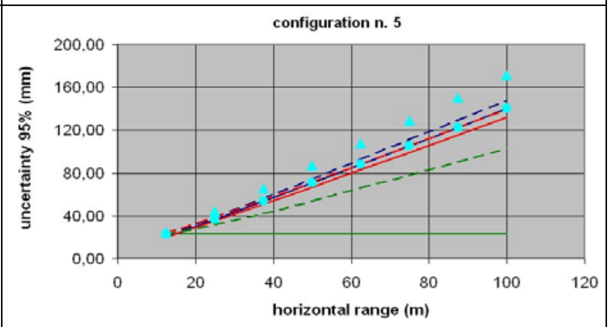
laser beam-width: 3 mrad σ_ρ= ± 10 mm $\sigma_{\alpha-\theta}$= ± 40 mgon	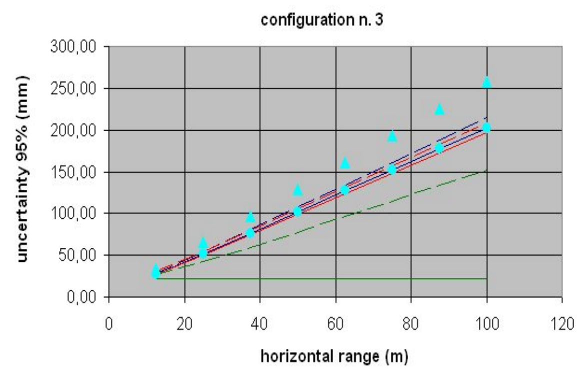	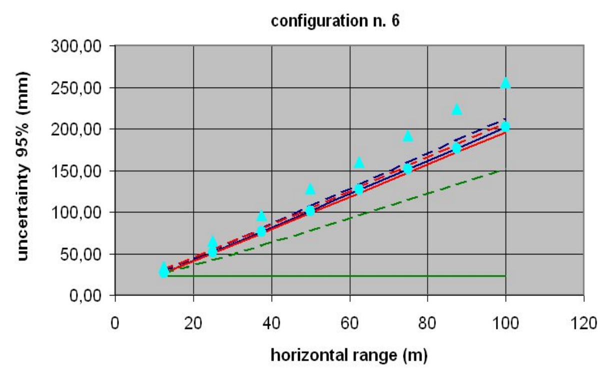
	Legend for vertical angle θ=0° sigmaX sigmaY sigmaZ sqrt(lambdama	Legend for vertical angle θ=40° sigmaX sigmaY sigmaZ sqrt(lambd

Figure 5 – Simulated coordinate accuracy from error propagation of different TLS configurations; two vertical angles for point positions have been considered.

Concerning the remaining parameters described at par. 4, we have established some fixed values that can be easily found in the practise. Consequently, the accuracy of stand-points has been fixed to ±5 mm for all coordinates, which have been considered uncorrelated. Trying different accuracies for stand-point coordinates has been omitted in tests, because in formula (13) the covariance matrix $\mathbf{C_0}$ is only an additive term and its effect can be easily evaluated. The uncertainty of instrumental height has been selected as $\sigma_{hs}=\pm3$ mm and that of stand-point centering as $\sigma_c=\pm1$ mm.The distance between the TLS stand-point and the orientation target has been always assumed as 30 m According to the formula for evaluting σ_κ in Table 1, this st.dev. is inversely proportional to the distance.

Results of tests are reported in graphics (Fig. 5) in term of 2σ precision (95% confidence) of 3D point coordinates in function of the horizontal distance from the scanner. In addition, the root of the maximum eigenvalue of the covariance matrix CX is shown, which makes this assessment independent from the adopted GRS.

The lecture of results which is presented in the following has been focused to assess the possibility of applying direct georeferencing in practical applications, omitting metrological analyses which have been already performed by the quoted authors.

5.2 Results on a real test: the church of S. Eufemia in Erba

A 3D model of the church of S. Eufemia in Erba (Italy) has been acquired by a Riegl LMS-Z420i instrument, equipped by the telescope (M=3) which is sold by the manufacturer as optional tool and by a level bubble of sensitivity v=30″. Moreover, data capture has been carried out by measuring some targets as well. The use of both direct and indirect georeferencing methods has shown some discrepancies in point cloud measurement. Differencies along a direction orthogonal to the surface have been estimated by comparing the surfaces of TIN models generated from both point cloud in planar areas; those in a parallel direction by finding a set of corresponding features, with the help of superimposed photo-texture. According to a maximum horizontal distance from object to TLS of about 55 m, discrepancies in coordinates of points have given R.M.S. in the order of 39 mm and 31 mm in the parallel plane and 25 mm in orthogonal direction. These findings show a similarity with respect to results of simulations for scanner configuration 1 (Fig. 5), accounting for the difficulty of making a comparison.

In Figure 6 the triangulated 3D model of S. Eufemia church is reported.

5.3 Main fields of application for direct georeferencing

Architectural surveying. The use of TLS tecnique for architectural survey can be finalized to obtain two main kinds of products: classical drawings such as planimetric maps, sections and prospects (i); *VR 3D-models* (ii). In both case the integration to photogrammetry is mandatory, due to the difficult interpretation of point cloud data and to the information augmentation achievable from imagery (see Beraldin, 2004).

Applications of group (i) require accuracies in the order of ±2÷3 cm (2σ), limiting the use of direct georeferencing only to high performance TLSs such as those in configuration 4 in Fig. 5. When operating in indoor environments, where distances more then 20-25 m rarely appear, also instruments such that in configuration 1 may be used. Considering the influence of single error sources to the total budget, the major contribute is due to uncertainty of stand-point and of azimuth determination. Improvements can be achieved by a higher precision geodetic network and by increasing the distance between scanner and orientation target.

In case of TLS survey for VR modeling, usually an accuracy about ±5÷10 cm is enough, according to the size of the site. For this kind of applications also scanner featuring configurations 2 and 3 might be applied, depending on the involved distances. When operating in outdoor environment large distances between scanning stations can be easily established, so that orientation targets must be placed as far as possible from the stand-point position to reduce the error on azimuth determination. On the contrary, in indoor projects the only way to reduce the uncertainty is to improve the network accuracy.

Figure 6 – The triangulated model of a portion of the Church of S. Eufemia in Erba (Italy) where a test on direct georeferencing has been performed.

5.3.2 Tunnel and indoor mine survey. We mention this specific application because here the direct georeferencing technique is highly suitable to be successfully applied. First of all, surveying in tunnels or mines is a very complex task due to adverse environmental conditions; the use of laser scanner instead of total stations might reduce the operating time, while the engagement of the operator is limited to control laser data acquisition and some total station measurements for geodetic network determination and for data integration. For the same grounds, avoiding the target positioning is a further advantage, calling for application of TLS direct georeferencing. Moreover, a high accuracy in 3D point coordinates is not required, due to the roughness of surfaces and to the aims of surveying, which are geometric modelling for static computation, design of protection structures, evaluation of excavated volumes, vizualization of dismissed mines for touristic and teaching purposes.

A point acquisition featuring an accuracy of about ±10 cm is enough for the most of applications. Considering that distances

from the scanner inside a mine or tunnel are usually very small (max 15÷20 m), every kind of TLS configuration in Figure 5 could be adopted.
To completely exploit the potential of TLS techniques, an instrument featuring a horizontal *panoramic* FoV and a vertical *semi-panoramic* FoV will further reduce the acquisition time. Example of such instruments are Leica HDS 3000 (360°x270° in two windows) and HDS 4500 (360°x320°), IQSun (360°x320°), VisImage (360°x270°), Zoller+Fröhlich IMAGER 5003 (360°x320°).
A more detailed analysis about this kind of applications can be found in Alba *et al.* (2005).

5.3.3 Road surveying. In this application the high operating speed, the mean accuracy in surface measurement (about ±5÷10 cm) and the possibility of integrating geometric data to imagery for a better interpretation of the derived model makes the laser scanner technique very suitable. Also in this case all instrumental configurations in Figure 5 may be used, according to the involved distances usually limited to 30÷40 m. It seems to be very promising the idea to equipe a *mobile mapping vehicle* by a laser scanner. Talaya *et al.* (2004) presented a vehicles where the scanner was integrated to a GPS/IMU system which allows to direct georeferencing each line scan when moving. The TLS is transformed so that in a line pushbroom scanner which is able to acquire measurements with an accuracy of ±20÷30 cm. We would like to propose a simpler solution, which however will improve the accuracy of 3D point measurement: the TLS is mounted on a mobile mapping vehicle and calibrated but not integrated to the GPS/IMU; when a road to be surveyed is reached, the vehicle is stopped and the data acquisition is started. Thank to the stationing time of a few minutes, more than one GPS epoques can be processed so that the positioning might reach a higher accuracy. The azimuth may be derived from the yaw angle measured by the IMU sensor or by installing a couple of GPS receivers.

6. FINAL CONSIDERATIONS

In the paper a background about direct TLS georeferencing has been presented, concerning either the geometric model for a general scanner mounting (also tilted) and the analysis of the whole error budget.
Some simulated and real tests have been carried out in order to evaluate the accuracy in data acquisition according to different sets of instrumental parameters. For each configuration, the accuracy of 3D point coordinate measurements has been evaluated as function of the distance from the scanner.
The first consideration is that the high performances reported by TLSs' vendors must be accurately verified, especially when using direct georeferencing. An accurate design of the surveying geometry is required, involving the need of highly skilled operators.
Nevertheless, some fields of applications exist where the use of direct georeferencing techniques seems to be very promising. These collect all cases where a relative medium-low accuracy in 3D point measurement, a rapidity of the surveying operations and the difficulty of target positioning are strictly required. We consider that the survey of architectural indoor environments, of tunnel, mines and roads as well as the data acquisition for VR modeling are applications where direct technique might give more fruitfull results in the near future.
Moreover, further investigations finalized to setup standard configurations for TLS data acquisition in such cases should be established, so that a large group of operators might afford with success these kinds of applications.

REFERENCES

References from Journals:

Fischler, M.A., and R.C. Bolles, 1981. Random Sample Consensus: a Paradigm for Model Fitting with Applications to Image Analysis and Automated Cartography. *Comm. ACM*, n. 24, pp. 381-395.

Gordon, S.J., and D.D. Lichti, 2004. Terrestrial laser scanners with a narrow field of view: the effect on 3D resection solutions. *Survey Review*, Vol. 37(292), 22 pp..

References from Other Literature:

Alba, M., Giussani, A., Roncoroni, F., and M. Scaioni, 2005. Strategies for Direct Georeferencing of Riegl LMS-Z420*i* Data. In printing in Proc. of *Optical 3D Measurement Techniques VII*, Vienna, Austria, 3-5 Oct.

Beinat, A., and F. Crosilla, 2001. Generalised Procrustes Analysis for Size and Shape 3-D Object Reconstructions. In Proc. of *Optical 3D Measurement Techniques V*, Vienna, Austria, 1-4 Oct, pp. 345-353.

Beraldin, J.A., 2004. Integration of Laser Scanning and Close-Range Photogrammetry – The Last Decade and Beyond. *IAPRSSIS*, Vol. 35(B7), Istambul, Turkey, pp. 972-983.

Fröhlich, C., and M. Mettenleiter, 2004. Terrestrial Laser Scanning – New Perspectives in 3D Surveying. *IAPRSSIS*, Vol. 36(8W2), Freiburg, Germany, pp. 7-13.

Grün, A., and D. Akca, 2004. Least Squares 3D Surface Matching. *IAPRSSIS*, Vol. 34(5/WG16), Dresden, Germany, on CDROM.

Lichti, D.D., and S.J. Gordon, 2004. Error Propagation in Directly Georeferenced Terrestrial Laser Scanner Point Clouds for Cultural Heritage Recording. In Proc. of *FIG Working Week*, Athens, Greece, May 22-27, pp. 16.

Scaioni, M., and G. Forlani, 2003. Independent Model Triangulation of Terrestrial Laser Scanner Data. *IAPRSSIS*, Vol. 34 (5/W12), Ancona Portonovo, Italy, pp. 308-313.

Talaya, J., Alamus, R., Bosch, E., Serra, A., Kornus, W., and A. Baron, 2004. Integration of a Terrestrial Laser Scanner with GPS/IMU Orientation Sensors. *IAPRSSIS*, Vol. 35(5), Istambul, Turkey,on DVD.

Ullrich, A., Schwarz, R., and H. Kager, 2003. Using Hybrid Multi-Station Adjustment for an Integrated Camera Laser-Scanner System. In Proc. of *Optical 3D Meas. Tech. VI*, Zurich, Switzerland, pp. 298-304.